

Probing the Interactions of O₂ with Small Gold Cluster Anions (Au_n⁻, n = 1–7): Chemisorption vs Physisorption

Wei Huang, Hua-Jin Zhai, and Lai-Sheng Wang*

Department of Chemistry, Brown University, Providence, Rhode Island 02912

Received December 9, 2009; E-mail: lai-sheng_wang@brown.edu

Abstract: Activation of O₂ is the most critical step in catalytic oxidation reactions involving gold and remains poorly understood. Here we report a systematic investigation of the interactions between O₂ and small gold cluster anions Au_n⁻ (n = 1–7) using photoelectron spectroscopy. Higher resolution photoelectron spectra are obtained for the molecularly chemisorbed even-sized Au_nO₂⁻ (n = 2, 4, 6) complexes. Well-resolved vibrational structures due to O–O stretching are observed and can be readily distinguished from the Au-derived PES bands. The adiabatic detachment energies and O–O vibrational frequencies are measured to be 3.03 ± 0.04, 3.53 ± 0.05, and 3.17 ± 0.05 eV, and 1360 ± 80, 1360 ± 80, and 1330 ± 80 cm⁻¹ for n = 2, 4, 6, respectively. Physisorbed Au_n(O₂) complexes for n = 1, 3, 5, 7 are observed for the first time, providing direct evidence for the inertness of the closed-shell odd-sized Au_n⁻ clusters toward O₂. Neutral even-sized Au_n clusters are closed-shell and are expected to be inert toward O₂, which is not consistent with the reduced O–O vibrational frequencies observed in the photoelectron spectra relative to free O₂. It is suggested that the photodetachment transitions can only access excited states of the neutral even-sized Au_nO₂ complexes; a double-well potential is proposed consisting of the ground-state van der Waals well at long Au_n–O₂ distances and a higher energy deeper well at short Au_n–O₂ distances derived from singlet O₂ (¹Δ_g). The current study provides further insight into O₂ interactions with small gold clusters, as well as accurate experimental data to benchmark theoretical investigations.

1. Introduction

The reactivity of gold clusters with O₂ is important for understanding the remarkable catalytic effects discovered for gold nanoparticles.¹ Bulk gold surfaces are known to be inactive toward O₂,² and thus O₂ activation is believed to be the main rate-limiting step in nanogold catalysis. While both anionic and cationic Au species have been proposed as active sites in nanogold catalysis,^{3–6} recent experimental evidence suggests that the catalytic active sizes for CO oxidation may involve subnanometer gold particles containing only about 10 Au atoms.⁷ Unsupported nanosized Au particles have also been shown to be active catalysts,^{8,9} suggesting that the catalytic

activity may be intrinsic to the nano- or subnanogold particles. A critical question pertaining to nanogold catalysis is whether and how gold nanoparticles interact with and activate molecular oxygen.

Size-selected gas phase clusters can serve as well-defined and controllable models for mechanistic understandings of nanogold catalysis at the molecular level.^{10–19} Early reactivity studies of Au_n⁻ toward O₂ revealed molecular O₂ addition as the primary reaction channel only for the even-sized clusters, whereas the odd-sized clusters are inert toward O₂.¹⁰ The even–odd alterna-

- (1) Haruta, M. *Catal. Today* **1997**, *36*, 153.
- (2) Gottfried, J. M.; Schmidt, K. J.; Schroeder, S. L. M.; Christmann, K. *Surf. Sci.* **2002**, *511*, 65.
- (3) (a) Sanchez, A.; Abbet, S.; Heiz, U.; Schneider, W. D.; Hakkinen, H.; Barnett, R. N.; Landman, U. *J. Phys. Chem. A* **1999**, *103*, 9573. (b) Yoon, B.; Hakkinen, H.; Landman, U.; Worz, A. S.; Antonietti, J. M.; Abbet, S.; Judai, K.; Heiz, U. *Science* **2005**, *307*, 403.
- (4) Yan, Z.; Chinta, S.; Mohamed, A. A.; Fackler, J. P., Jr.; Goodman, D. W. *J. Am. Chem. Soc.* **2005**, *127*, 1604.
- (5) (a) Guzman, J.; Gates, B. C. *J. Am. Chem. Soc.* **2004**, *126*, 2672. (b) Fierro-Gonzalez, J. C.; Bhirud, V. A.; Gates, B. C. *Chem. Commun.* **2005**, 5275.
- (6) Fu, Q.; Saltsburg, H.; Flytzani-Stephanopoulos, M. *Science* **2003**, *301*, 935.
- (7) Herzing, A. A.; Kiely, C. J.; Carley, A. F.; Landon, P.; Hutchings, G. J. *Science* **2008**, *321*, 1331.
- (8) Iizuka, Y.; Tode, T.; Takao, T.; Yatsu, K. I.; Takeuchi, T.; Tsubota, S.; Haruta, M. *J. Catal.* **1999**, *187*, 50.
- (9) Xu, C.; Su, J.; Xu, X.; Liu, P.; Zhao, H.; Tian, F.; Ding, Y. *J. Am. Chem. Soc.* **2007**, *129*, 42.

- (10) (a) Cox, D. M.; Brickman, R. O.; Creegan, K.; Kaldor, A. Z. *Phys. D* **1991**, *19*, 353. (b) Lee, T. H.; Ervin, K. M. *J. Phys. Chem.* **1994**, *98*, 10023. (c) Salisbury, B. E.; Wallace, W. T.; Whetten, R. L. *Chem. Phys.* **2000**, *262*, 131.
- (11) (a) Hagen, J.; Socaciu, L. D.; Eljazyfer, M.; Heiz, U.; Bernhardt, T. M.; Woste, L. *Phys. Chem. Chem. Phys.* **2002**, *4*, 1707. (b) Bernhardt, T. M. *Int. J. Mass Spectrom.* **2005**, *243*, 1.
- (12) Wallace, W. T.; Whetten, R. L. *J. Am. Chem. Soc.* **2002**, *124*, 7499.
- (13) Socaciu, L. D.; Hagen, J.; Bernhardt, T. M.; Woste, L.; Heiz, U.; Hakkinen, H.; Landman, U. *J. Am. Chem. Soc.* **2003**, *125*, 10437.
- (14) (a) Stolcic, D.; Fischer, M.; Gantefor, G.; Kim, Y. D.; Sun, Q.; Jena, P. *J. Am. Chem. Soc.* **2003**, *125*, 2848. (b) Kim, Y. D.; Fischer, M.; Gantefor, G. *Chem. Phys. Lett.* **2003**, *377*, 170.
- (15) Sun, Q.; Jena, P.; Kim, Y. D.; Fischer, M.; Gantefor, G. *J. Chem. Phys.* **2004**, *120*, 6510.
- (16) Kimble, M. L.; Castleman, A. W., Jr.; Mitric, R.; Burgel, C.; Bonacic-Koutecky, V. *J. Am. Chem. Soc.* **2004**, *126*, 2526.
- (17) Fielicke, A.; von Helden, G.; Meijer, G.; Pedersen, D. B.; Simard, B.; Rayner, D. M. *J. Am. Chem. Soc.* **2005**, *127*, 8416.
- (18) (a) Zhai, H. J.; Wang, L. S. *J. Chem. Phys.* **2005**, *122*, 051101. (b) Zhai, H. J.; Kiran, B.; Dai, B.; Li, J.; Wang, L. S. *J. Am. Chem. Soc.* **2005**, *127*, 12098.
- (19) (a) Neumaier, M.; Weigend, F.; Hampe, O.; Kappes, M. M. *J. Chem. Phys.* **2005**, *122*, 104702. (b) Neumaier, M.; Weigend, F.; Hampe, O.; Kappes, M. M. *Faraday Discuss.* **2008**, *138*, 393.

tion correlates well with a similar trend in the electron affinities of Au_n,²⁰ suggesting that electron transfer from Au_n[−] to O₂ might be the primary reaction mechanism.^{10c} In subsequent photoelectron spectroscopy (PES) studies,^{14,15} spectroscopic evidence was reported, showing that the even-sized Au_nO₂[−] clusters are indeed molecularly chemisorbed complexes via the observation of O–O vibrational structures, with estimated vibrational spacings ranging from ~180 meV (1450 cm^{−1}) for *n* = 2 and 6 to 152 meV (1230 cm^{−1}) for *n* = 4.

There have been numerous theoretical investigations on the reactivity of gold clusters with O₂. While most theoretical studies show the even–odd effect for the anion clusters, consistent with the experimental observations, the situation for the neutral clusters is more complicated because there is a lack of direct experimental probe for the uncharged species. Several previous density functional theory (DFT) studies show persistently that neutral Au clusters interact with O₂ rather weakly, insufficient to activate molecular oxygen.^{21,22} Specifically, Landman and co-workers²¹ concluded that, despite the weak binding to O₂, neutral and cationic Au clusters do not induce O–O bond activation. Jena and co-workers¹⁵ showed that in neutral Au₂O₂ and Au₄O₂ clusters electron transfer takes place from O₂ to Au₂ and Au₄ owing to the high electronegativity of Au. Ding et al.²² showed that there is no O₂ chemisorption in the Au_nO₂ (*n* = 2, 4, 6) neutral complexes, and thus their O–O stretching frequencies should be close to or almost the same as that in free O₂ (1580 cm^{−1}). *Ab initio* calculations by the groups of Gordon and Metiu showed that while O₂ has a 1.07 eV binding energy to Au₂[−] it only weakly interacts with either Au₃[−] or Au₃.²³ They showed that DFT methods can give rise to large errors in predicting the O₂ binding to gold clusters.

However, the consistent theoretical predictions of weak binding between O₂ and neutral gold clusters do not agree with the observed vibrational structures in the PES spectra of even-sized Au_nO₂[−] (*n* = 2, 4, 6) complexes.¹⁴ Since PES probes the final neutral states, the observed vibrational structures should be due to the O–O vibration in the *neutral* Au_nO₂ (*n* = 2, 4, 6) complexes. The reduced O–O frequencies relative to free O₂ in the PES spectra are puzzling. Clearly, there is something significant that is not well understood about the O₂ interactions with small gold clusters. High-quality spectroscopic data are needed to provide further insight.

In the current article, we report a systematic PES study of the Au_nO₂[−] (*n* = 1–7) complexes for both the even- and odd-sized clusters. For the even-sized clusters (*n* = 2, 4, 6), significantly better resolved spectra are obtained and the possible mechanisms for the observed reduced O–O frequencies are discussed. For the odd-sized clusters (*n* = 1, 3, 5, 7), physisorbed Au_n[−](O₂) complexes are observed for the first time and their PES spectra are nearly identical to those of the parent Au_n[−] clusters, providing direct spectroscopic evidence for the inertness of these clusters toward O₂. For AuO₂[−] and Au₃O₂[−], both the dioxide forms and the O₂ complexes are observed when an O₂/He carrier gas is used, whereas only the dioxide forms are

observed when a N₂O/He carrier gas is used. The current results provide further insight into the mechanisms of O₂ activation by small gold clusters and can be used to benchmark high-level computational studies on the interactions of O₂ with Au clusters.

2. Experimental Method

The experiment was carried out using a magnetic-bottle PES apparatus equipped with a laser vaporization cluster source, details of which have been described previously.²⁴ Briefly, the Au_nO₂[−] cluster complexes were produced by laser vaporization of a pure Au disk target in the presence of a He carrier gas seeded with different amounts of O₂ and analyzed using a time-of-flight mass spectrometer. The Au_nO₂[−] (*n* = 1–7) clusters of current interest were each mass-selected and decelerated before being photodetached. The photodetachment experiments were performed at three photon energies: 355 nm (3.496 eV), 266 nm (4.661 eV), and 193 nm (6.424 eV). Effort was made to control cluster temperatures and to choose colder clusters for photodetachment, which has proved essential for obtaining high-quality PES data.²⁵ Photoelectrons were collected at nearly 100% efficiency by the magnetic bottle and analyzed in a 3.5 m long electron flight tube. The experiment was run at 20 Hz repetition rate with the cluster beam off at alternating laser shots for background subtraction. Photoelectron time-of-flight spectra were converted to kinetic energy (Ek) spectra, calibrated using the known spectra of Au[−] and Rh[−]. The reported electron-binding energy spectra were obtained by subtracting the kinetic energy spectra from the respective photon energies. The energy resolution of the PES apparatus was ΔEk/Ek ≈ 2.5%, that is, ~25 meV for 1 eV electrons.

We found that in our cluster source the cluster distributions depended strongly on the O₂ content in the He carrier gas. At 0.1% O₂, we observed only Au_nO₂[−] complexes with even *n* in the size range of *n* = 2–8, consistent with previous studies.^{10,14} At 0.5% O₂, we found that most of the even-sized Au_n[−] clusters were converted to the Au_nO₂[−] complexes. At the same time, more extensive O-containing clusters (Au_nO_x[−]) were observed, including odd-numbered *n* and *x*. At 5% O₂, we observed nearly continuous cluster distributions of Au_nO_x[−] in both *n* and *x* due to extensive oxidation and complex formation. Most of our PES experiments were done using the 0.5% O₂/He carrier gas. For AuO₂[−], we used 5% O₂/He carrier gas to enhance its intensity. We also used N₂O-seeded He carrier as the O source and were able to observe AuO₂[−] and Au₃O₂[−], which were compared with the results from the O₂-seeded carrier gas.

3. Results

3.1. Au_nO₂[−] (*n* = 2, 4, 6). The PES spectra of Au_nO₂[−] (*n* = 2, 4, 6) at 193 nm are compared with those of the corresponding bare Au_n[−] clusters in Figure 1. Higher resolution spectra at 266 nm for Au_nO₂[−] are shown in Figure 2. The new data are consistent with the previous reports by Gantefor and co-workers,¹⁴ but are better resolved. In the 193 nm spectra (Figure 1), weak and broad features are observed in the low binding energy side, which come primarily from detachment from the O₂[−] unit in Au_nO₂[−]. The relatively sharp features at higher binding energies (>4.8 eV) originate from the Au cluster substrates. At 266 nm (Figure 2), only the O₂-derived bands are observed, which are resolved into different vibrational progressions. In the 266 spectrum of Au₂O₂[−] (Figure 2a), three vibrational progressions (X, A, B) are resolved with frequencies

(20) Taylor, K. J.; Pettiette-Hall, C. L.; Cheshnovsky, O.; Smalley, R. E. *J. Chem. Phys.* **1992**, *96*, 3319.

(21) Yoon, B.; Hakkinen, H.; Landman, U. *J. Phys. Chem. A* **2003**, *107*, 4066.

(22) (a) Ding, X.; Li, Z.; Yang, J. L.; Hou, J. G.; Zhu, Q. *J. Chem. Phys.* **2004**, *120*, 9594. (b) Ding, X.; Dai, B.; Yang, J. L.; Hou, J. G.; Zhu, Q. *J. Chem. Phys.* **2004**, *121*, 621.

(23) (a) Varganov, S. A.; Olson, R. M.; Gordon, M. S.; Metiu, H. *J. Chem. Phys.* **2003**, *119*, 2531. (b) Mills, G.; Gordon, M. S.; Metiu, H. *Chem. Phys. Lett.* **2002**, *359*, 493.

(24) Wang, L. S.; Cheng, H. S.; Fan, J. *J. Chem. Phys.* **1995**, *102*, 9480.

(25) (a) Wang, L. S.; Li, X. In *Clusters and Nanostructure Interfaces*; Jena, P.; Khanna, S. N.; Rao, B. K., Eds.; World Scientific: NJ, 2000; pp 293–300. (b) Akola, J.; Manninen, M.; Hakkinen, H.; Landman, U.; Li, X.; Wang, L. S. *Phys. Rev. B* **1999**, *60*, R11297.

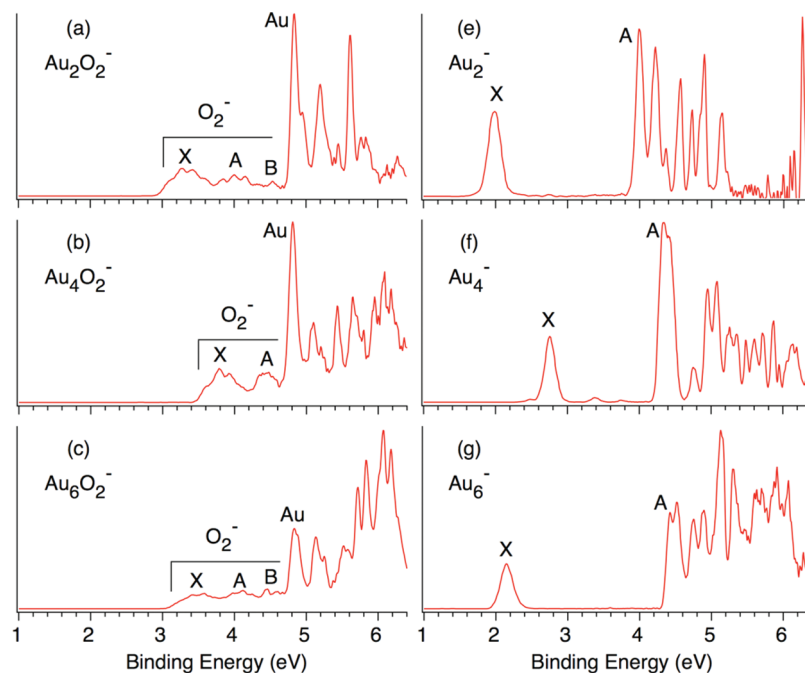


Figure 1. Photoelectron spectra of even-sized Au_nO_2^- ($n = 2, 4, 6$) at 193 nm (6.424 eV) in comparison with those of the corresponding Au_n^- clusters.

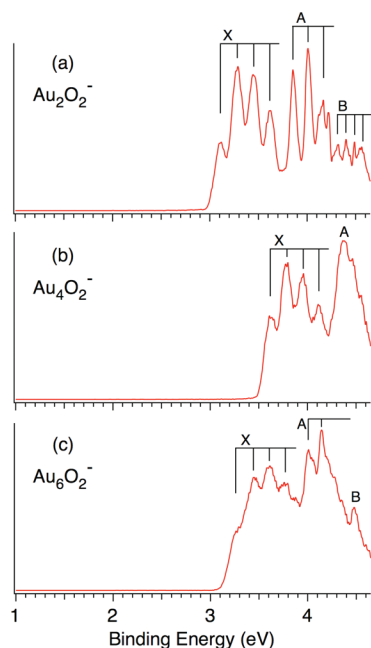


Figure 2. Photoelectron spectra of Au_nO_2^- ($n = 2, 4, 6$) at 266 nm (4.661 eV). Resolved vibrational structures are labeled.

of 1360, 1250, and ~ 700 cm^{-1} , respectively. In the 266 nm of Au_4O_2^- (Figure 2b), two bands are observed, where the X band is vibrationally resolved. For Au_6O_2^- (Figure 2c), three bands are observed and vibrational structures are resolved in the X and A bands. The B band in the spectra of Au_2O_2^- and Au_6O_2^- was not identified in the previous study due to lower spectral resolution and poor signal-to-noise ratios.¹⁴ However, because of the photon energy cutoff at 266 nm and the difficulty in detecting low-energy electrons by the magnetic-bottle PES analyzer, the spectral intensity above 4.5 eV in Figure 2 is not reliable. Nevertheless, as will be discussed in Section 4.2, the O_2^- -derived spectral features in Au_nO_2^- ($n = 2, 4, 6$) resemble

Table 1. Observed Adiabatic (ADE) and Vertical (VDE) Detachment Energies and O–O Vibrational Frequencies from the PES Spectra of Au_nO_2^- ($n = 2, 4, 6$)^a

	feature	ADE (eV)	VDE (eV)	vib freq (cm^{-1})
Au_2O_2^-	X	3.03 (4)	3.29 (5)	1360 (70)
	A	3.86 (4)	4.01 (5)	1250 (70)
	B	4.32 (5)	~ 4.54	~ 700
	Au		4.84 (4)	
Au_4O_2^-	X	3.53 (5)	3.78 (5)	1360 (80)
	A		4.37 (5)	
Au_6O_2^-	X	3.17 (5)	3.61 (5)	1330 (100)
	A	4.01 (5)	4.15 (5)	1100 (80)
	B	4.48 (5)	>4.48	
	Au		4.83 (4)	

^a Numbers in parentheses represent the experimental uncertainties in the last digits.

those of free O_2^- , and the assignment of the B band in the spectra of the $n = 2$ and 6 species in the current study is sound.

From the vibrationally resolved spectra, the vertical detachment energy (VDE) for the ground-state transition in each case is readily obtained from the most intense vibrational peak, as summarized in Table 1, where the ground-state vibrational frequencies are also given. However, the vibrational peaks of band X in each spectrum show a width of about 120–140 meV, which is much larger than the instrumental resolution. This large spectral width can be due to either contributions from unresolved low-frequency vibrational modes or lifetime broadening. Therefore, the ground-state adiabatic detachment energy (ADE) is estimated by drawing a straight line along the leading edge of the first vibrational peak in each case and then adding the instrumental resolution to the intersection with the binding energy axis. The obtained ADE values are also given in Table 1 for Au_nO_2^- ($n = 2, 4, 6$).

3.2. AuO_2^- . The 193 nm spectra of AuO_2^- are shown in Figure 3 at different source conditions and compared with that of Au^- . The spectrum in Figure 3a is obtained with a 1% N_2O -seeded He carrier gas. This spectrum is entirely due to the linear O^-AuO^- dioxide, which has been studied in detail in a recent

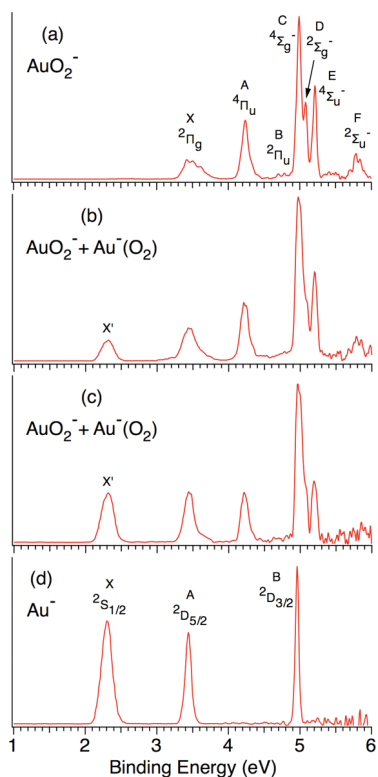


Figure 3. Photoelectron spectra of AuO₂⁻ at 193 nm in comparison with that of Au⁻. (a) Spectrum of AuO₂⁻ dioxide using a N₂O/He carrier gas; the assignments are from ref 26. (b and c) Spectra of AuO₂⁻ using an O₂/He carrier gas, showing contributions of the Au⁻(O₂) van der Waals complex, whose intensities increase with better cooling from (b) to (c).

joint PES and *ab initio* study.²⁶ The spectral assignments obtained from the previous study are given in Figure 3a. The spectrum shown in Figure 3b is measured for AuO₂⁻ produced using 5% O₂/He as the carrier gas. This spectrum is different from the data in Figure 3a: an extra peak (X') around 2.3 eV is observed and at the same time the relative intensity of the X band for the AuO₂⁻ dioxide appears to be enhanced. As we increase the cooling effect of the cluster source, we observe the relative intensity of the X' band increases (Figure 3c).

As described previously,²⁵ the cluster temperatures from our source depend on the residence time inside the cluster nozzle. The longer the residence time, the colder the clusters. We can tune the residence time or the relative cluster temperatures by varying the delay time of the cluster extraction for mass analyses with respect to the firing of the vaporization laser. A smaller delay time implies a short residence time or hot clusters. In Figure S1, we show a series of spectra for AuO₂⁻ produced with the 5% O₂/He carrier gas at different residence times. We observe that under hot conditions only the AuO₂⁻ dioxide isomer is produced. As we increase the residence time, the extra peak gradually appears and becomes very strong at the longest residence time. These observations suggest that the extra peak comes from a weakly bound or physisorbed Au⁻(O₂) complex. Indeed, the X' peak of Au⁻(O₂) is nearly the same as that of Au⁻ (Figure 3d). The second and third peaks from the Au⁻(O₂) complex should also be similar to those (A and B) of Au⁻, and they overlap with the X and C bands of AuO₂⁻ dioxide,

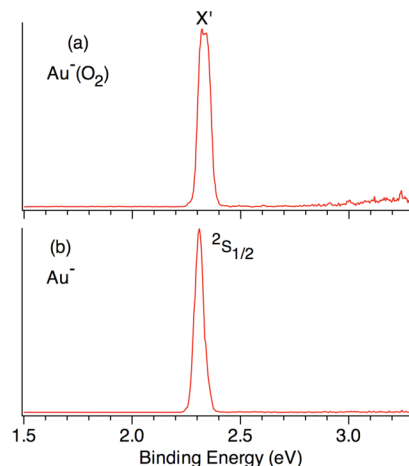


Figure 4. Photoelectron spectrum of the Au⁻(O₂) van der Waals complex at 355 nm (3.496 eV) in comparison with that of Au⁻.

Table 2. Observed Adiabatic Detachment Energies (ADE) of Physisorbed O₂ Complexes for the Odd-Sized Clusters, Au_n⁻(O₂) (n = 1, 3, 5, 7), Compared with Those of the Corresponding Free Au_n⁻ Clusters^a

Au _n ⁻ (O ₂)	ADE	Au _n ⁻	ADE ^b	ΔE ^c
1	2.322 (10)	1	2.30863	0.013
3	3.89 (1)	3	3.88 (2)	0.01
5	3.10 (2)	5	3.08 (3)	0.02
7	3.42 (3)	7	3.42 (3)	~0

^a All values are in eV. Numbers in parentheses represent the uncertainties in the last digits. ^b The ADE of Au⁻ is from ref 36, and those for the larger clusters are from ref 27. ^c Shift of the ADE of Au_n⁻(O₂) relative to that of Au_n⁻.

respectively, as can be seen by comparing Figure 3, c and d. We further measured the spectrum of the physisorbed Au⁻(O₂) complex with enhanced resolution at 355 nm (Figure 4a), which displays unresolved fine features. The ADE of Au⁻(O₂) is measured to be 2.322 eV (Table 2), which is slightly higher than that of Au⁻ (2.3086 eV) and is consistent with the weakly bound nature of Au⁻(O₂).

3.3. Au₃O₂⁻. The 193 nm spectra of Au₃O₂⁻ under different source conditions are compared with that of bare Au₃⁻ in Figure 5. The spectrum shown in Figure 5b was obtained for Au₃O₂⁻ using a 1% N₂O/He carrier gas under similar conditions to those for the AuO₂⁻ dioxide spectrum in Figure 3a. This spectrum displays extremely high electron-binding energies, with the VDE of the X band being 4.32 eV. Similar to the AuO₂⁻ dioxide, this Au₃O₂⁻ species must be also in the dioxide form. The spectrum in Figure 5c was obtained by using the 0.5% O₂/He carrier gas. The Au₃O₂⁻ system behaves similarly to AuO₂⁻: in addition to the dioxide form, a weak low-binding energy peak (X', Figure 5c) appears at ~3.9 eV. The binding energy of this peak is very similar to that of bare Au₃⁻, suggesting that this peak comes from a physisorbed Au₃⁻(O₂) similar to Au⁻(O₂). However, the relative intensity of the Au₃⁻(O₂) complex is always weak even under the coldest source conditions. In Figure 6, we compare the 266 nm spectra of Au₃O₂⁻ and Au₃⁻ under higher spectral resolution. The relative intensity of the X' band is much enhanced. The ADE of the Au₃⁻(O₂) complex is measured to be 3.89 eV (Table 2), slightly blue-shifted relative to that of Au₃⁻ (3.88 eV), consistent with the weakly bonded nature of Au₃⁻(O₂). The A band of Au₃⁻ exhibited a dramatic photon energy dependence, and its relative intensity was

(26) Zhai, H. J.; Burgel, C.; Bonacic-Koutecky, V.; Wang, L. S. *J. Am. Chem. Soc.* **2008**, *130*, 9156.

(27) Hakkinen, H.; Yoon, B.; Landman, U.; Li, X.; Zhai, H. J.; Wang, L. S. *J. Phys. Chem. A* **2003**, *107*, 6168.

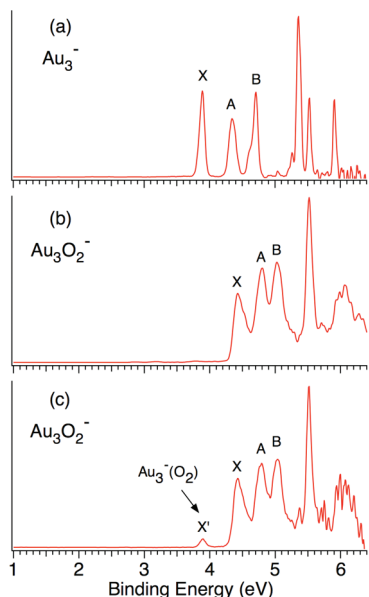


Figure 5. Photoelectron spectra of Au_3O_2^- at 193 nm in comparison with that of Au_3^- (a). (b) Spectrum of Au_3O_2^- using a $\text{N}_2\text{O}/\text{He}$ carrier gas. (c) Spectrum of Au_3O_2^- using an O_2/He carrier gas, showing contributions from a weakly bonded $\text{Au}_3^-(\text{O}_2)$ complex.

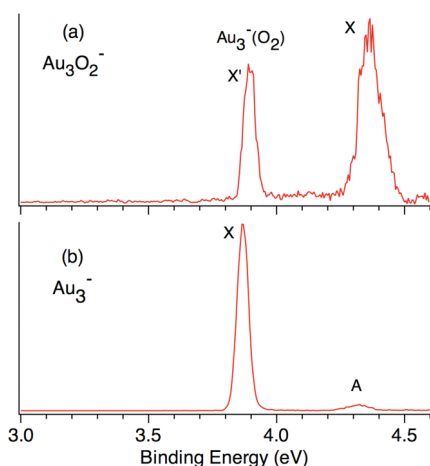


Figure 6. Photoelectron spectrum of the weakly bonded $\text{Au}_3^-(\text{O}_2)$ complex at 355 nm in comparison with that of Au_3^- .

significantly reduced at 266 nm (Figure 6b), as pointed out previously.²⁷

3.4. Au_5O_2^- and Au_7O_2^- . The spectra of Au_5O_2^- and Au_7O_2^- at two different photon energies are compared with their parent gold clusters in Figures 7 and 8, respectively. We observe the spectra of Au_5O_2^- and Au_7O_2^- to be nearly identical to their respective parent gold clusters. Even the ADE of each O_2 complex displays no measurable shift from its parent gold clusters within our experimental uncertainties (Table 2). These observations suggest that these two clusters exist in the form of weakly bonded van der Waals complexes, $\text{Au}_5^-(\text{O}_2)$ and $\text{Au}_7^-(\text{O}_2)$, in which O_2 exerts little perturbation to the parent gold clusters. We have also produced van der Waals clusters of Au_n^- with Ar and obtained their PES spectra, which are all identical to those of the parent gold clusters with little spectral shift.²⁸ There are some very weak signals in the spectra of the O_2 complexes, notably between 3.5 and 4.0 eV in the case of $\text{Au}_5^-(\text{O}_2)$ (Figure 7a) and between 4.0 and 4.4 eV in the case of $\text{Au}_7^-(\text{O}_2)$ (Figure 8a). These weak signals could come from

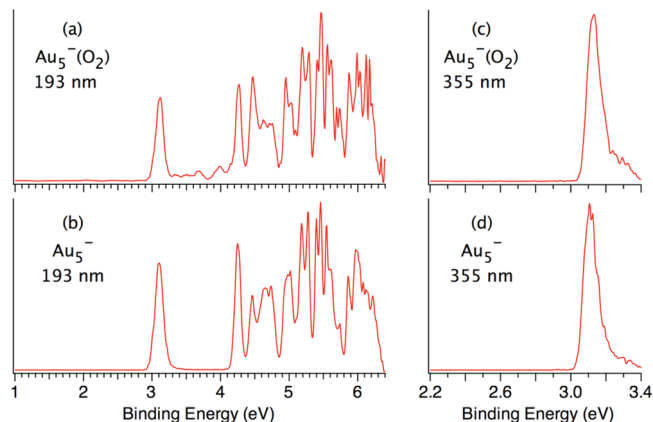


Figure 7. Photoelectron spectra of weakly bonded $\text{Au}_5^-(\text{O}_2)$ complex at 193 and 355 nm in comparison with those of Au_5^- .

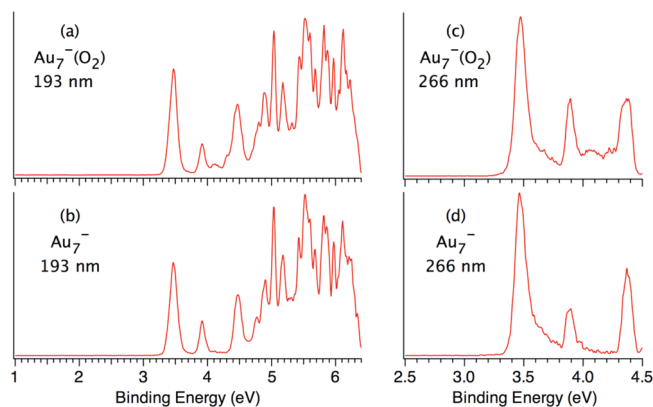


Figure 8. Photoelectron spectra of weakly bonded $\text{Au}_7^-(\text{O}_2)$ complex at 193 and 355 nm in comparison with those of Au_7^- .

minor populations of the dioxide isomers. However, using the $\text{N}_2\text{O}/\text{He}$ carrier gas, we observed negligible intensities for the dioxides in these cases.

4. Discussion

4.1. Physisorption of O_2 to Odd-Sized Au_n^- ($n = 1, 3, 5, 7$) Clusters. The observation of physisorbed $\text{Au}_n^-(\text{O}_2)$ complexes for the odd-sized clusters is a vivid demonstration of the inertness of these closed-shell gold cluster anions toward O_2 . The dioxide isomers of AuO_2^- and Au_3O_2^- are formed, respectively, by reactions of Au^- and Au_3^- with O atoms, which can be produced in the laser vaporization plasma. This conclusion is confirmed by the experiment using N_2O as the oxygen source. Although the AuO_2^- dioxide is more stable than the $\text{Au}^-(\text{O}_2)$ complex, it cannot be formed by direct reactions of Au^- with O_2 . Jena and co-workers showed using DFT calculations that there is a 3 eV barrier for the $\text{Au}^- + \text{O}_2$ reaction to form the dioxide,¹⁵ which cannot be overcome under thermal conditions. The physisorbed nature of the $\text{Au}^-(\text{O}_2)$ complex has been recently studied in detail, showing that the O_2 binding energy to Au^- is only about 0.03 eV (0.78 kcal/mol) at the CCSD(T) level and the complete basis set limit.²⁹ Bonacic-

- (28) (a) Huang, W.; Wang, L. S. *Phys. Chem. Chem. Phys.* **2009**, *11*, 2663. (b) Huang, W.; Wang, L. S. *Phys. Rev. Lett.* **2009**, *102*, 153401. (c) Huang, W.; Bulusu, S.; Pal, R.; Zeng, X. C.; Wang, L. S. *ACS Nano* **2009**, *3*, 1225.
(29) Gao, Y.; Huang, W.; Woodford, J.; Wang, L. S.; Zeng, X. C. *J. Am. Chem. Soc.* **2009**, *131*, 9484.

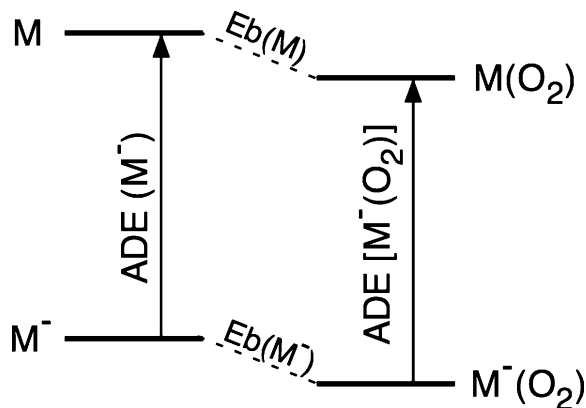


Figure 9. Schematics showing the relationship between adiabatic detachment energies (ADE) of anions and the O₂ binding energies (Eb) for a neutral and anion cluster.

Koutecky and co-workers have calculated the structure of the Au₃O₂⁻ dioxide,³⁰ which possesses a bent geometry and can be viewed as a Au₂ dimer end-bonded to a linear AuO₂⁻ dioxide. Similar to the AuO₂⁻ dioxide, the Au₃O₂⁻ dioxide is not formed by direct reactions of Au₃⁻ with O₂.

Previous DFT calculations suggest that the O₂ binding energies to the odd-sized Au_n⁻ clusters (n = 3, 5, 7) range from 0.3 to 0.6 eV.^{21–23} However, using the CCSD(T) level of theory the groups of Gordon and Metiu have shown that in fact O₂ does not bind to Au₃⁻ and that DFT methods tend to overestimate the O₂ binding to gold clusters.^{23a} The CCSD(T) result is confirmed by the current experimental observation: the Au₃⁻(O₂) complex was difficult to observe, and it could be formed only under our coldest source conditions. For Au₅⁻ and Au₇⁻, the O₂ binding must be also very weak because O₂ has very little effect on the electronic structures of the parent clusters. In particular, O₂ does not even induce a shift in the ADE of Au₇⁻(O₂) relative to that of Au₇⁻, suggesting that the interactions between O₂ and Au₇⁻ or Au₇ are similar and equally weak (Figure 9). As shown in Table 2, for n = 1, 3, 5, the O₂ binding induces a small blue shift in the ADEs of the Au_n⁻(O₂) complexes relative to those of the bare clusters. These results imply that O₂ interacts with the anions slightly more strongly than with the corresponding neutral clusters, i.e., Eb(M⁻) > Eb(M) in Figure 9, because Eb(M⁻) = Eb(M) + ADE[M⁻(O₂)] – ADE(M⁻). Available calculations in the literature are not consistent in predicting this binding energy trend from the anion to the neutral for the odd-sized clusters. In fact, the majority of the available calculations suggest that O₂ binds more strongly to the neutral odd-sized gold clusters than to the anions, inconsistent with the current experimental observations. As schematically shown in Figure 9, if O₂ were to bind more strongly to the neutral clusters, the observed ADEs for the Au_n⁻(O₂) complexes should be smaller than those for their corresponding Au_n⁻ clusters.

4.2. Molecular Chemisorption of O₂ on Even-Sized Au_n⁻ Clusters in Au_nO₂⁻ (n = 2, 4, 6). From a careful saturation chemisorption study, Whetten and co-workers suggested that the interaction between even-sized Au_n⁻ clusters and O₂ is via a one-electron charge transfer,^{10c} yielding adsorbed superoxide complexes, Au_n(O₂⁻). The observation of O–O vibrational structures in the PES of Au_nO₂⁻ (n = 2, 4, 6) by Gantefor and

co-workers confirmed this interpretation.¹⁴ In the current study, we observed clearly three electronic transitions in the case of Au₂O₂⁻ (X, A, B), which are due to the O₂⁻ moiety. These three bands are in fact reminiscent of the photoelectron spectrum of free O₂⁻,³¹ providing further electronic structure evidence for the charge transfer interaction in the even-sized Au_nO₂⁻ clusters.

Free molecular O₂ possesses an open-shell triplet ³Σ_g⁻ ground state with the antibonding π_g orbital half-filled (π_g²). In O₂⁻, the extra electron enters the π_g orbital, resulting in the ²Π_g ground state for O₂⁻ (π_g³). Photodetachment from O₂⁻ results in the triplet ³Σ_g⁻ ground state and two low-lying excited singlet states for O₂, ¹Δ_g and ¹Σ_g⁺, with excitation energies at 0.982 and 1.636 eV, respectively.³¹ As shown in Figure 2a and Table 1, the 266 nm PES spectrum of Au₂O₂⁻ yields excitation energies of 0.83 and 1.29 eV for the A and B bands, respectively. Different from those reported by Gantefor et al., the current higher resolution data show that the vibrational frequencies and the excitation energies in all three systems are nearly identical, as shown in Figure S2, where the 266 nm spectra of Au_nO₂⁻ (n = 2, 4, 6) are aligned for comparison. Note that only two O₂-derived PES bands (X and A) are observed for Au₄O₂⁻ at 266 nm (Figure 2b) because of its high electron-binding energies. Another interesting observation is that the onsets of the Au-derived PES features are identical for all three systems (4.81–4.83 eV) within our experimental uncertainty, as seen in Figure 1a–c.

4.3. On the Inconsistency of the Observed O–O Vibrational Frequencies in the PES Spectra of the Even-Sized Au_nO₂⁻ (n = 2, 4, 6) Clusters and the Expected Inertness of the Corresponding Neutral Au_n Clusters with O₂. Previous experimental studies have shown that the closed-shell odd-sized Au_n⁻ clusters do not react with O₂.¹⁰ Our current observations of weakly bonded O₂ complexes of these clusters provide direct spectroscopic evidence for the inertness of the odd-sized Au_n⁻ clusters toward O₂. The closed-shell Au_n⁻ clusters possess relatively high electron-binding energies, making it energetically unfavorable for the charge transfer reaction to O₂. Besides the high electron-binding energies, the spin selection rule also makes the closed-shell Au_n⁻ clusters unfavorable to react with O₂, which has a triplet ground state as mentioned above. A recent study has shown that closed-shell aluminum Al_n⁻ cluster anions react much more slowly with O₂, but their reactivity is considerably enhanced with singlet O₂ (¹Δ_g).^{32a} Interestingly, both the global minimum D_{3h} Au₁₀⁻ and the Au₁₆⁻ cage are known to be unreactive to O₂:^{10,28a} they are exceptions to the even–odd effect in the Au_n⁻ reactivity with O₂, although they possess the same spin state as the other reactive even-sized Au_n⁻ clusters. These two clusters possess high electron-binding energies as a result of their corresponding neutrals being open-shell triplet states.^{27,33} Again, the spin selection rule may also play a role in the nonreactivity of Au₁₀⁻ and Au₁₆⁻ with O₂. Recently, we have observed a weakly bonded Au₁₀⁻(O₂) complex, which yields a PES spectrum identical to that of the parent D_{3h} Au₁₀⁻ and confirms the inertness of Au₁₀⁻ toward O₂.^{28a}

(30) Kimble, M. L.; Moore, N. A.; Johnson, G. E.; Castleman, A. W.; Burgel, C.; Mitric, R.; Bonacic-Koutecky, V. *J. Chem. Phys.* **2006**, *125*, 204311.

(31) Buntine, M. A.; Lavrich, D. J.; Dessent, C. E.; Scarton, M. G.; Johnson, M. A. *Chem. Phys. Lett.* **1993**, *216*, 471.

(32) (a) Burgert, R.; Schnockel, H.; Grubisic, A.; Li, X.; Stokes, S. T.; Bowen, K. H.; Gantefor, G. F.; Kiran, B.; Jena, P. *Science* **2008**, *319*, 438. (b) Reber, A. C.; Khanna, S. N.; Roach, P. J.; Woodward, W. H.; Castleman, A. W. *J. Am. Chem. Soc.* **2007**, *129*, 16098.

(33) Bulusu, S.; Li, X.; Wang, L. S.; Zeng, X. C. *Proc. Natl. Acad. Sci. U.S.A.* **2006**, *103*, 8326.

Analogously, the closed-shell neutral Au_n clusters ($n = 2, 4, 6$) are not expected to react with O_2 because the electron-binding (ionization) energies in these neutral clusters are much higher than those for the closed-shell odd-sized Au_n^- cluster anions. In other words, the neutral closed-shell Au_n clusters should form only weakly bonded physisorbed complexes with O_2 . This conclusion is clearly inconsistent with the PES spectra of $Au_nO_2^-$, which yield spectroscopic information about the neutral Au_nO_2 final states. The O–O vibrational frequency of 1360 cm^{-1} observed in the PES spectra for the ground states of all three Au_nO_2 systems is significantly smaller than that for free O_2 (1580 cm^{-1}). The vibrational frequency of the superoxide ion, O_2^- , is 1090 cm^{-1} .³⁴ The 1360 cm^{-1} vibrational frequency observed for the ground states of neutral Au_nO_2 complexes is between those of the free O_2 and O_2^- , suggesting significant chemical interactions between Au_n and O_2 in the final Au_nO_2 states, accessed in the photodetachment transitions.

As discussed in the Introduction, previous calculations have also shown that neutral Au_n clusters do not activate O_2 . Then, the question is, how does one understand the reduced O–O vibrational frequency in the neutral Au_nO_2 final states in the photodetachment experiment of $Au_nO_2^-$ ($n = 2, 4, 6$)?

4.4. Access of Excited States in PES of $Au_nO_2^-$ ($n = 2, 4, 6$). According to our experimental observation of the weakly bonded nature of the closed-shell anions, the interactions between the even-sized Au_n clusters and O_2 should be extremely weak and should be represented by a shallow van der Waals well. The O–O vibrational frequencies in the weakly bonded $Au_n(O_2)$ complexes should be close to that of free O_2 . Since PES is a vertical process, it may not be able to access the ground-state van der Waals potential curve of $Au_n(O_2)$. A detachment transition to the van der Waals well would be a bound-to-unbound transition, which should yield very broad and diffused PES bands. Instead, the observed PES spectra suggest bound-to-bound transitions, which could result only from transitions to excited states of Au_nO_2 . This observation suggests that the interactions between Au_n and O_2 may correspond to a double-well potential with a shallow ground-state van der Waals well at long Au_n-O_2 distances and a deeper well at closer Au_n-O_2 distances, but at a higher energy. The higher energy, deeper well can result from interactions of Au_n with an excited state of O_2 and an avoided curve crossing with the ground-state van der Waals well, resulting in the putative double-well potential for Au_nO_2 , as schematically shown in Figure 10.

The excited state could come from the interaction of Au_n with singlet O_2 ($^1\Delta_g$) (Figure 10), which is well known to be much more reactive than the ground-state triplet O_2 ($^3\Sigma_g^-$).³⁵ In addition, the spin-state selection rule is also fulfilled between the reactions of the singlet O_2 and the closed-shell Au_n clusters. The first detachment channel reaching the $Au_n-O_2(^1\Delta_g)$ final state can be understood from the following consideration. In the $Au_n(O_2^-)$ complexes, the degeneracy of the π_g orbital in the O_2^- moiety is expected to be lifted, resulting in two nondegenerate orbitals: a fully occupied orbital (a^2) and a singly occupied orbital (SOMO) (b^1), as schematically shown in Figure 11a. A single electron detachment from the SOMO of $Au_n(O_2^-)$ would result in a final state of $Au_n(O_2)$ corresponding to the $^1\Delta_g$ state of free O_2 , as schematically shown in Figure 11b. Detachment of a spin-down electron from the a^2 orbital would result in a

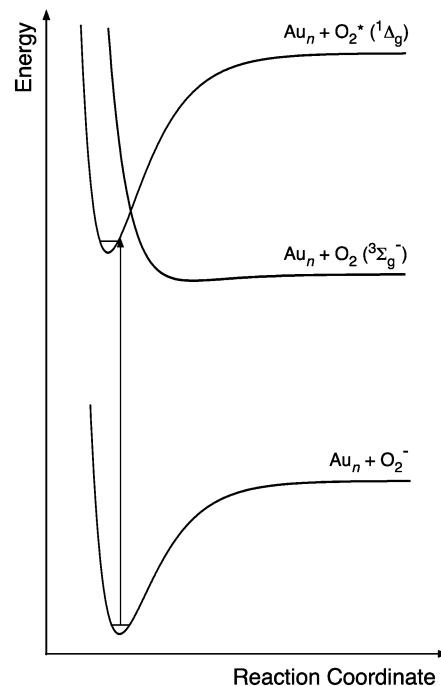


Figure 10. Schematic potential energy curves illustrating vertical detachment transitions from the ground state of $Au_nO_2^-$ ($n = 2, 4, 6$) to the final neutral states of Au_nO_2 . Note the curve crossing between the ground-state van der Waals well and the deeper well between Au_n and the singlet O_2 ($^1\Delta_g$), which would result in a double well due to avoided curve crossing.

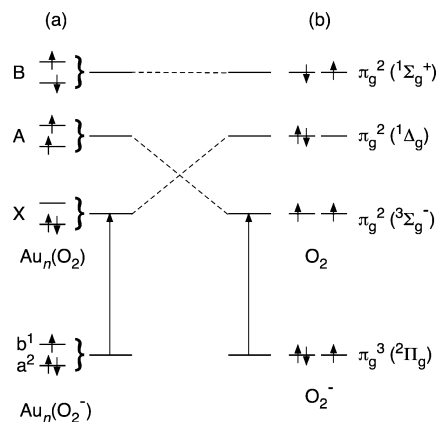


Figure 11. Schematics correlating single electron detachment from the O_2^- moiety in $Au_nO_2^-$ ($n = 2, 4, 6$) with those from free O_2^- .

triplet final state in $Au_n(O_2)$, which should correspond to the $^3\Sigma_g^-$ state of free O_2 . This detachment channel should reach the repulsive part of the ground-state Au_n-O_2 van der Waals well (Figure 10), corresponding to the A band in the PES spectra. The observed vibrational structures in the A band suggest a transition to a bound state, which is likely derived from the avoided curve crossing with the potential energy curve from the $^1\Delta_g$ state of O_2 . The detachment of a spin-up electron from the a^2 orbital should lead to a final state corresponding to the $^1\Sigma_g^+$ state of free O_2 (Figure 11).

The deeper well in the double-well potential in $Au_n(O_2)$ is unstable, and predissociation occurs to the ground state. This is consistent with our observed 266 nm photoelectron spectra (Figure 2), in which the resolved vibrational peaks are all much broader than the instrumental resolution. While this broadening can be due to unresolved low-frequency vibrational modes, one

(34) NIST Chemistry WebBook: <http://webbook.nist.gov/chemistry>.

(35) Schweitzer, C.; Schmidt, R. *Chem. Rev.* **2003**, *103*, 1685.

(36) Riestra-Kiracife, J. C.; Tschumper, G. S.; Schaefer, H. F.; Nandi, S.; Ellison, G. B. *Chem. Rev.* **2002**, *102*, 231.

possibility would be lifetime broadening due to predissociation to the ground state, providing evidence for the proposed interpretation.

Ab initio calculations at the CCSD(T) level showed that DFT calculations tend to overestimate the Au_n⁻/O₂ binding by as much as 0.5 eV,^{23a} which is on the order of the interactions between gold clusters and O₂. Preliminary calculations by Jun Li (private communication) suggest that there is significant multireference character in the ground state wave function of Au₂O₂⁻. Therefore, the interactions between O₂ and gold clusters are quite complicated. The current data should provide good benchmarks to calibrate theoretical methods that can properly treat the O₂ interactions with gold clusters. It would also be very interesting to investigate the reactivities of singlet oxygen with gold clusters to confirm the proposed double-well potential for the interactions of O₂ with neutral gold clusters.

5. Conclusions

In conclusion, we present a systematic PES study of the Au_nO₂⁻ (n = 1–7) cluster complexes. Well-resolved photoelectron spectra are obtained for the even-sized Au_nO₂⁻ (n = 2, 4, 6) clusters, confirming the molecular chemisorption nature of O₂ in these systems. Both the electron-binding energies and O–O vibrational frequencies are more accurately measured. Physisorbed Au_n⁻(O₂) complexes are observed for the odd-sized Au_nO₂⁻ (n = 1, 3, 5, 7) clusters for the first time, confirming the inertness of the odd-sized Au_n⁻ clusters toward O₂. The inconsistency of the observed O–O vibrational frequency with

the expected inertness of the even-sized *neutral* Au_n clusters toward O₂ is discussed. It is suggested that photodetachment from the molecularly chemisorbed Au_n(O₂⁻) complexes cannot access the ground-state van der Waals potential curves of the *neutral* even-sized Au_n(O₂) complexes. A double-well potential is proposed for the Au_n–O₂ interaction, which consists of a lower energy, shallow van der Waals well at long Au_n–O₂ distances and a higher energy, deeper well at shorter Au_n–O₂ distances. The double-well potential is suggested to result from a putative avoided curve crossing between the ground-state van der Waals well and the deeper well derived from interactions of Au_n with singlet O₂ (¹Δ_g). Clearly more accurate theoretical calculations are needed to understand the PES spectra and the detailed interactions between O₂ and gold clusters. Such understanding is important for elucidating the catalysis of supported gold nanoparticles, in which the activation of O₂ is the most important step.

Acknowledgment. We thank Professors Jun Li, Mingfei Zhou, and Manfred Kappes for valuable discussions. This research was supported by the National Science Foundation (CHE-0749496).

Supporting Information Available: Photoelectron spectra of AuO₂⁻ at 193 nm under different experimental conditions and comparison of the fine features in the 266 nm photoelectron spectra of Au_n(O₂⁻) (n = 2, 4, 6). This material is available free of charge via the Internet at <http://pubs.acs.org>.

JA910401X